Transactions on Power Systems, Vol. 7, No. 2, May 1992

POINT OF COLLAPSE METHODS APPLIED TO AC/DC POWER SYSTEMS

Claudio A. Cañizares, Student Member, IEEE
Fernando L. Alvarado, Senior Member, IEEE
Christopher L. DeMarco, Member, IEEE
Ian Dobson, Member, IEEE
Willis F. Long, Fellow, IEEE
University of Wisconsin–Madison
Madison, Wisconsin 53706 USA

Abstract: This paper describes an extension of the Point of Collapse method developed for ac systems studies to the determination of saddle-node bifurcations in power systems including high voltage direct current (HVDC) transmission. Bus voltage profiles are illustrated for an ac/dc test system, which significantly differ from the profiles of pure ac systems for typical system models. In particular, voltage dependent current order limits (VDCOLs) are shown to affect the voltage profiles ("nose" curves) and the loadability margin of the system. It is also shown that Hopf bifurcations, which are not possible in purely ac lossless systems with second-order generator models, become plausible when the dynamics for the HVDC system are included.

Keywords: Voltage collapse, HVDC, singularity, point of collapse, saddle-node bifurcations, Hopf bifurcations.

INTRODUCTION

Voltage instability and collapse have been observed in several electric power networks throughout the world, and have been the subject of increasing study over the past few years [1]. Furthermore, the relative wide spread use of HVDC systems for the transmission of large amounts of power [2, 3, 4, 5] has motivated several researchers to study voltage stability issues in ac/dc systems by using voltage sensitivity factors (VSFs) [6, 7]. The VSF has been shown not to be a good measure of proximity to collapse in ac systems [1], especially for buses with large amounts of reactive support. This paper analyzes the problem using bifurcation theory of nonlinear systems to determine the distance in state space to the point of collapse, so that better estimates of the loadability margins of the ac/dc system can be obtained.

Here some of the mathematical and computational tools for voltage stability studies in ac systems are extended to incorporate HVDC models, and to gain new insight into the nature of the voltage collapse problem in ac/dc systems. Moreover, the paper discusses some of the difficulties encountered during the calculation of the unstable equilibrium points (i.e., additional solutions of the power flow equations corresponding to unstable eigenvalues of the linearized ac/dc system dynamic equations), which have proven useful in voltage stability analysis of ac systems [8, 9].

This paper is organized as follows. The assumptions and models representing the ac/dc system transient behavior are first presented. Next, the mathematical background describing bifurcation (voltage collapse) phenomena for the ac/dc system equations is discussed. Numerical techniques used to locate the loading levels that correspond to the bifurcation point are also described. Finally, these techniques are applied to a reduced ac/dc sample system.

91 SM 491-1 PWRS A paper recommended and approved by the IEEE Power System Engineering Committee of the IEEE Power Engineering Society for presentation at the IEEE/PES 1991 Summer Meeting, San Diego, California July 28 - August 1, 1991. Manuscript submitted January 29, 1991; made available for printing May 8, 1991.

SYSTEM MODELS AND ASSUMPTIONS

The ac system is represented using transient stability models that assume quasi-static evolution of bus voltage phasors on the time scale of interest [5].

Generators (n_G)

Voltage V_g sources behind transient reactance X'_d are used, and q-axis transient voltage dynamics are included. Generator n_G is the system reference ($\delta_{n_G} = 0$).

$$\begin{aligned}
\dot{\delta}_g &= \omega_g - \omega_{n_G} \\
\dot{\omega}_g &= \frac{1}{M_g}\left(P_m^0 - P_{gt} - D_g\omega_g\right) \\
\dot{V}_g &= \frac{X_d - X'_d}{T'_{d_o}}\left[\frac{E_f - V_g}{X_d - X'_d} - \frac{V_g}{X'_d} + \frac{V_t}{X'_d}\cos(\delta_t - \delta_g)\right] \\
P_{gt} &= \frac{V_g V_t}{X'_d}\sin(\delta_g - \delta_t) \\
Q_{gt} &= -\frac{V_t^2}{X'_d} + \frac{V_g V_t}{X'_d}\cos(\delta_g - \delta_t)
\end{aligned} \tag{1}$$

Here P_{gt} and Q_{gt} are the powers injected by the generator at bus t. E_f represents the field voltage, and X_d stands for the synchronous generator reactance. While E_f is held constant in these equations, more detailed exciter dynamics can be easily added.

Transmission System

A constant admittance model (G, B, B_s) is employed.

$$\begin{aligned}
P_{sr} &= GV_s^2 - GV_sV_r\cos(\delta_s - \delta_r) \\
&\quad + BV_sV_r\sin(\delta_s - \delta_r) \\
Q_{sr} &= (B_s + B)V_s^2 - GV_sV_r\sin(\delta_s - \delta_r) \\
&\quad - BV_sV_r\cos(\delta_s - \delta_r)
\end{aligned} \tag{2}$$

Here P_{sr} and Q_{sr} are the transmitted powers from bus s to bus r.

0885-8950/92$03.00©1992 IEEE

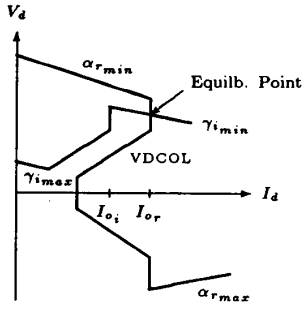

Fig. 1: *HVDC control criteria. Notice that the rectifier is allowed to go into inverter operation for faster recovery after fault conditions.*

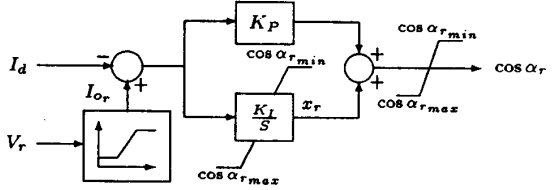

Fig. 2: *PI rectifier current controller. The inverter side has a similar control circuit.*

Loads (n_L)

Voltage and frequency dependent load models are employed.

$$\begin{aligned} P_l &= P_{l_1}\left(\frac{V_l}{V_l^0}\right)^2 + P_{l_2}\left(\frac{V_l}{V_l^0}\right) + P_{l_3} \\ &\quad + D_l(\dot{\delta}_l + \omega_{n_G}) + \lambda\Delta P_l \\ Q_l &= Q_{l_1}\left(\frac{V_l}{V_l^0}\right)^2 + Q_{l_2}\left(\frac{V_l}{V_l^0}\right) + Q_{l_3} + \lambda\Delta Q_l \end{aligned} \tag{3}$$

Here P_l and Q_l are the powers absorbed by the load at bus l, and λ is a parameter used to simulate the slow time scale load variation that drives the system to collapse. D_l is the load frequency coefficient (a time constant in seconds).

HVDC (n_{dc})

A variation of typical control schemes is used to represent the HVDC converter behavior in quasi-static operation (Fig. 1). This scheme can be realized using the control circuit depicted in Fig. 2. Notice that the VDCOL is modelled as a nonlinear function of the converter ac bus voltage.

The HVDC link as represented here has basically two different control regimes. Under normal operating conditions, the rectifier controller controls the current while the inverter current controller remains saturated (and therefore "out of the loop"). However, when the system experiences a fault condition, the rectifier controller can be driven into saturation while the inverter controller "takes over" the current control. The HVDC system can be modelled, under normal operating conditions and assuming ideal harmonic filtering, by [2, 3, 4, 5]:

$$\dot{I}_d = \frac{1}{L_d}(V_{d_r} - V_{d_i}) - \frac{R_d}{L_d} I_d \tag{4}$$

$$\begin{aligned} \dot{x}_r &= K_I[I_{o_r}(V_r) - I_d] \\ \cos\alpha_r &= x_r + K_P[I_{o_r}(V_r) - I_d] \\ V_{d_r} &= \frac{3\sqrt{2}}{\pi} a_r V_r \cos\alpha_r - \frac{3}{\pi} X_{c_r} I_d \\ S_r &= \frac{V_n I_n}{S_n}\frac{3\sqrt{2}}{\pi} a_r V_r I_d \\ P_r &= \frac{V_n I_n}{S_n} V_{d_r} I_d \\ Q_r &= \sqrt{S_r^2 - P_r^2} \\ \cos\gamma_i &= \cos\gamma_{i_{min}} \\ V_{d_i} &= \frac{3\sqrt{2}}{\pi} a_i V_i \cos\gamma_i - \frac{3}{\pi} X_{c_i} I_d \\ S_i &= \frac{V_n I_n}{S_n}\frac{3\sqrt{2}}{\pi} a_i V_i I_d \\ P_i &= -\frac{V_n I_n}{S_n} V_{d_i} I_d \\ Q_i &= \sqrt{S_i^2 - P_i^2} \end{aligned}$$

Here V_{d_r} and V_{d_i} are the per unit dc terminal voltages at the rectifier and inverter ends, respectively. I_n (kA) and V_n (kV) are the base quantities for the dc system, and S_n is the base power in MVA for the ac side. X_{c_r} and X_{c_i} are the per unit commutation reactances, and R_d and L_d are the per unit dc line parameters. The products $a_r V_r$ and $a_i V_i$ are the per unit ac bus voltages at the secondary side of the transformers with respect to the dc bus voltage base V_n. S_r and S_i are the per unit magnitudes of the HVDC complex powers at the ac side, and P_r, P_i, Q_r and Q_i are the per unit active and reactive powers absorbed by the dc system. When the inverter takes over current control, the equations for $\dot{x}_r$, $\cos\alpha_r$, and $\cos\gamma_i$ are replaced by:

$$\begin{aligned} \dot{x}_i &= K_I[I_d - I_{o_i}(V_i)] \\ \cos\gamma_i &= x_i + K_P[I_d - I_{o_i}(V_i)] \\ \cos\alpha_r &= \cos\alpha_{r_{min}} \end{aligned} \tag{5}$$

These equations are valid, within a roughly 4% error margin, for overlap angles μ_r and μ_i of up to 60^0, i.e., there is a (three-valve) commutation every 60^0 in a six-pulse bridge. They are not valid for four-valve commutation, since under these operating conditions the dc link must be represented by a different set of equations [5].

The controller model is such that inverter current control and rectifier current control typically do not overlap. For high rectifier voltages and/or low inverter voltages the rectifier current controller is in operation while the inverter controller is saturated at its minimum value $\gamma_{i_{min}}$; conversely, for low rectifier voltages and/or high inverter voltages the roles of inverter and rectifier controllers are reversed. During recovery from fault conditions it is typical to have both converters controlling the current for a brief period. Each one of these cases is represented by "switching" to the appropriate set of differential equations.

The following vectors are defined for rectifier current control at each HVDC link ($k = 1, 2, \cdots, n_{dc}$):

$$\begin{aligned} \mathbf{x}_{dc_k} &= [x_{r_k}\ I_{d_k}]^T \\ \mathbf{y}_{dc_k} &= [\cos\alpha_{r_k}\ V_{d_{r_k}}\ S_{r_k}\ \cos\gamma_{i_k}\ V_{d_{i_k}}\ S_{i_k}]^T \\ \mathbf{V}_{dc_k} &= [V_{r_k}\ V_{i_k}]^T \end{aligned}$$

$$\begin{aligned}\mathbf{P}_{dc_k} &= [P_{r_k}\ P_{i_k}]^T \\ \mathbf{Q}_{dc_k} &= [Q_{r_k}\ Q_{i_k}]^T\end{aligned}$$

These vectors change when the inverter controls the dc current. In either case equations (4) can be rewritten as:

$$\begin{aligned}\dot{\mathbf{x}}_{dc_k} &= \mathbf{h}_{dc_k}(\mathbf{V}_{dc_k}, \mathbf{x}_{dc_k}, \mathbf{y}_{dc_k}) \\ \mathbf{0} &= \mathbf{w}_{dc_k}(\mathbf{V}_{dc_k}, \mathbf{x}_{dc_k}, \mathbf{y}_{dc_k}) \\ \mathbf{P}_{dc_k} &= \mathbf{f}_k(\mathbf{V}_{dc_k}, \mathbf{x}_{dc_k}, \mathbf{y}_{dc_k}) \\ \mathbf{Q}_{dc_k} &= \mathbf{g}_k(\mathbf{V}_{dc_k}, \mathbf{x}_{dc_k}, \mathbf{y}_{dc_k})\end{aligned} \tag{6}$$

Vector Equations

Equations (1) to (5) can be arranged into vector differential equations (7) for an n bus ac/dc system ($n = n_G + n_L + 2n_{dc}$). The vectors $\mathbf{f}(\cdot)$ and $\mathbf{g}(\cdot)$ stand for normalized ac active and reactive power flow mismatch equations, respectively, and $\mathbf{V} = [\mathbf{V}_G^T\ \mathbf{V}_L^T\ \mathbf{V}_{dc}^T]^T$ and $\delta = [\delta_G^T\ \delta_L^T\ \delta_{dc}^T]^T$. To simplify the eigenvalue analysis, the reference generator n_G is assumed to be an infinite bus. The analysis does not lose generality since system equilibria require that $\omega_{n_G} = 0$.

$$\begin{aligned}\dot{\mathbf{x}}_{dc} &= \mathbf{h}_{dc}(\mathbf{V}_{dc}, \mathbf{x}_{dc}, \mathbf{y}_{dc}) \\ \dot{\delta}_G &= \omega_G \\ \mathbf{M}_G\dot{\omega}_G &= \mathbf{f}_G(\delta, \mathbf{V}) - \mathbf{D}_G\omega_G \\ \mathbf{D}_x\dot{\mathbf{V}}_G &= \mathbf{g}_G(\delta, \mathbf{V}) \\ \mathbf{D}_L\dot{\delta}_L &= \mathbf{f}_L(\delta, \mathbf{V}, \lambda) \\ \mathbf{0} &= \begin{bmatrix} \mathbf{g}_L(\delta, \mathbf{V}, \lambda) \\ \mathbf{f}_{dc}(\delta, \mathbf{V}, \mathbf{x}_{dc}, \mathbf{y}_{dc}) \\ \mathbf{g}_{dc}(\delta, \mathbf{V}, \mathbf{x}_{dc}, \mathbf{y}_{dc}) \end{bmatrix} \\ \mathbf{0} &= \mathbf{w}_{dc}(\mathbf{V}_{dc}, \mathbf{x}_{dc}, \mathbf{y}_{dc})\end{aligned} \tag{7}$$

Matrices $\mathbf{M}_G$, $\mathbf{D}_G$, $\mathbf{D}_x$, and $\mathbf{D}_L$ are all positive definite diagonal constant matrices.

BIFURCATIONS AND EIGENVALUES

It will prove convenient to define a composite vector that groups all state variables defined by the differential equations, and a second vector that groups all variables defined by the algebraic constraints. Let $\mathbf{z} = [\mathbf{x}_{dc}^T\ \delta_G^T\ \omega_G^T\ \mathbf{V}_G^T\ \delta_L^T]^T$, and $\mathbf{u} = \left[[\mathbf{V}_L^T\ \delta_{dc}^T\ \mathbf{V}_{dc}^T]\ \mathbf{y}_{dc}^T\right]^T$. Similarly, define a composite vector function, $\hat{\mathbf{f}}(\cdot)$, that groups all the terms representing the right hand side of differential equations, and a composite vector function, $\hat{\mathbf{g}}(\cdot)$, that groups all terms representing algebraic constraints. When the algebraic constraints $\hat{\mathbf{g}}(\cdot)$ have an invertible Jacobian $D_u\hat{\mathbf{g}}_\lambda$ along the system trajectories of interest, the algebraic variables can be eliminated (Implicit Function Theorem [10]), and (7) reduces to:

$$\left.\begin{aligned}\mathbf{M}\,\dot{\mathbf{z}} &= \hat{\mathbf{f}}_\lambda(\mathbf{z}, \mathbf{u}) \\ \mathbf{0} &= \hat{\mathbf{g}}_\lambda(\mathbf{z}, \mathbf{u})\end{aligned}\right\} \quad \mathbf{M}\,\dot{\mathbf{z}} = \hat{\mathbf{f}}_\lambda(\mathbf{z}, \hat{\mathbf{h}}_\lambda(\mathbf{z})) = \mathbf{s}(\mathbf{z}, \lambda) \tag{8}$$

where $\mathbf{M}$ is a positive definite diagonal constant matrix.

A bifurcation [11, 12], or structural instability, occurs when the Jacobian $D_z\mathbf{s}(\cdot)$ of (8) is singular at the equilibrium $(\mathbf{z}_0, \lambda_0)$. Several types of bifurcation are possible in this situation, but of these only the saddle-node bifurcation occurs generically so that it is expected to be typical in practice [11, 13]. (More formally: a general one parameter family of differential equations such as (8) with singular Jacobian at an equilibrium can be perturbed to produce saddle-node bifurcations, and saddle-node bifurcations are robust to perturbations in the model.) The saddle-node is characterized by 2 equilibria coalescing and then disappearing as the parameter (e.g., load power) increases. Moreover the following conditions [11] generically apply at $(\mathbf{z}_0, \lambda_0)$:

1. $D_z\mathbf{s}(\mathbf{z}_0, \lambda_0)$ has a simple and unique zero eigenvalue, with right eigenvector $\mathbf{v}$ and left eigenvector $\mathbf{w}$, i.e., $D_z\mathbf{s}(\mathbf{z}_0, \lambda_0)\,\mathbf{v} = \mathbf{0}$ and $\mathbf{w}^T D_z\mathbf{s}(\mathbf{z}_0, \lambda_0) = \mathbf{0}$.

2. $$\mathbf{w}^T \left.\frac{\partial \mathbf{s}}{\partial \lambda}\right|_{(\mathbf{z}_0, \lambda_0)} \neq 0. \tag{9}$$

3. $$\mathbf{w}^T \left[D_z^2\mathbf{s}(\mathbf{z}_0, \lambda_0)\,\mathbf{v}\right]\mathbf{v} \neq 0. \tag{10}$$

In equation (10) the square bracketed product of the 3-tensor $D_z^2\mathbf{s}\big|_0$ and the eigenvector $\mathbf{v}$ yields a matrix.

Conditions 1 through 3 guarantee generic quadratic behavior (i.e., two solutions joining into one) near the bifurcation point, and also prevent singularities of the composite Jacobian in the Newton-Raphson based method for finding saddle-nodes described below. Examples of such saddle-nodes occurring in ac/dc systems are illustrated in the sample system to follow.

An important computational issue in bifurcation studies for power systems is the relationship between eigenvalues of the power flow Jacobian $\mathbf{J}_{PF}$ and those of the system dynamics linearized at the equilibrium point, denoted by $\mathbf{J}_{TS} = \mathbf{M}^{-1}D_z\mathbf{s}(\mathbf{z}_0, \lambda_0)$. This subject has been examined for simpler system models in [14, 15, 16]. The following discussion demonstrates that singularity (zero eigenvalue) of the power flow Jacobian implies a zero eigenvalue for the linearized system dynamics. Linearizing $\hat{\mathbf{f}}(\cdot)$ and $\hat{\mathbf{g}}(\cdot)$ at the equilibrium yields a block Jacobian of the form:

$$D(\hat{\mathbf{f}}, \hat{\mathbf{g}})|_0 = \left[\begin{array}{c|c} D_z\hat{\mathbf{f}}_\lambda|_0 & D_u\hat{\mathbf{f}}_\lambda|_0 \\ \hline D_z\hat{\mathbf{g}}_\lambda|_0 & D_u\hat{\mathbf{g}}_\lambda|_0 \end{array}\right]$$

Eliminating the algebraic variables yields the Jacobian for the reduced dynamic system, i.e.,

$$\mathbf{M}\,\mathbf{J}_{TS} = D_z\hat{\mathbf{f}}_\lambda|_0 - D_u\hat{\mathbf{f}}_\lambda|_0 D_u\hat{\mathbf{g}}_\lambda|_0^{-1} D_z\hat{\mathbf{g}}_\lambda|_0$$

which can be shown to have the following structure:

$$\mathbf{M}\,\mathbf{J}_{TS} = \begin{array}{c|ccccc} & \mathbf{x}_{dc} & \delta_G & \omega_G & \mathbf{V}_G & \delta_L \\ \hline \dot{\mathbf{x}}_{dc} & \mathbf{P}_1 & \mathbf{P}_2 & \mathbf{0} & \mathbf{P}_3 & \mathbf{P}_4 \\ \dot{\delta}_G & \mathbf{0} & \mathbf{0} & \mathbf{I}_{n_G-1} & \mathbf{0} & \mathbf{0} \\ \mathbf{M}_G\dot{\omega}_G & \mathbf{P}_5 & \mathbf{P}_6 & -\mathbf{D}_G & \mathbf{P}_7 & \mathbf{P}_8 \\ \mathbf{D}_x\dot{\mathbf{V}}_G & \mathbf{P}_9 & \mathbf{P}_{10} & \mathbf{0} & \mathbf{P}_{11} & \mathbf{P}_{12} \\ \mathbf{D}_L\dot{\delta}_L & \mathbf{P}_{13} & \mathbf{P}_{14} & \mathbf{0} & \mathbf{P}_{15} & \mathbf{P}_{16} \end{array}$$

Then, using standard block determinant formulas, the determinant of $\mathbf{J}_{TS}$ can be calculated:

$$\begin{aligned}\det\mathbf{J}_{TS} &= (-1)^k \det\mathbf{M}^{-1} \det \begin{vmatrix} \mathbf{P}_1 & \mathbf{P}_2 & \mathbf{P}_3 & \mathbf{P}_4 \\ \mathbf{P}_5 & \mathbf{P}_6 & \mathbf{P}_7 & \mathbf{P}_8 \\ \mathbf{P}_9 & \mathbf{P}_{10} & \mathbf{P}_{11} & \mathbf{P}_{12} \\ \mathbf{P}_{13} & \mathbf{P}_{14} & \mathbf{P}_{15} & \mathbf{P}_{16} \end{vmatrix} \\ &= (-1)^k \frac{\det\mathbf{P}}{\det\mathbf{M}}\end{aligned} \tag{11}$$

where k is a positive integer.

On the other hand, the power flow Jacobian can be obtained from (7) with $\omega_G = 0$, and it can be shown that:

$$\det \mathbf{J}_{PF} = \det \mathbf{P} \, \det D_u \hat{\mathbf{g}}_\lambda|_0 \tag{12}$$

Hence, from (11) and (12):

$$\det \mathbf{J}_{TS} = (-1)^k \frac{\det \mathbf{J}_{PF}}{\det \mathbf{M} \, \det D_u \hat{\mathbf{g}}_\lambda|_0} \tag{13}$$

Thus, it suffices to look for zero eigenvalues of $\mathbf{J}_{PF}$ in order to identify singularities of the full linearized dynamics.

THE POINT OF COLLAPSE METHOD

This technique augments the equations for equilibria with constraints ensuring a zero eigenvalue at the point of interest. This approach is described by Seydel [12], and was applied to voltage stability analysis of ac systems in [17]. The equations for $\mathbf{z}$, $\mathbf{v}$, and λ take the following form:

$$\begin{aligned} \mathbf{s}(\mathbf{z}, \lambda) &= \mathbf{0} \\ D_z \mathbf{s}(\mathbf{z}, \lambda)\, \mathbf{v} &= \mathbf{0} \\ \mathbf{v} &\neq \mathbf{0} \end{aligned} \tag{14}$$

Solving (14) is equivalent to solving equations (15) below for $\tilde{\mathbf{z}} = [\mathbf{x}_{dc}^T \ \delta_G^T \ \mathbf{V}_G^T \ \delta_L^T]^T$, $\mathbf{u}$, $\hat{\mathbf{v}}$, and λ, since under the assumption of $D_u \hat{\mathbf{g}}_\lambda|_0$ invertible, singularity of the "power flow" Jacobian is necessary and sufficient for singularity of $D_z \mathbf{s}$.

$$\begin{aligned} \begin{bmatrix} \tilde{\mathbf{f}}_\lambda(\tilde{\mathbf{z}}, \mathbf{u}) \\ \hat{\mathbf{g}}_\lambda(\tilde{\mathbf{z}}, \mathbf{u}) \end{bmatrix} &= \mathbf{0} \\ \begin{bmatrix} D_{\tilde{z}} \tilde{\mathbf{f}}_\lambda & D_u \tilde{\mathbf{f}}_\lambda \\ D_{\tilde{z}} \hat{\mathbf{g}}_\lambda & D_u \hat{\mathbf{g}}_\lambda \end{bmatrix} \begin{bmatrix} \hat{\mathbf{v}}_{\tilde{z}} \\ \hat{\mathbf{v}}_u \end{bmatrix} &= \mathbf{0} \\ \begin{bmatrix} \hat{\mathbf{v}}_{\tilde{z}} \\ \hat{\mathbf{v}}_u \end{bmatrix} &\neq \mathbf{0} \end{aligned} \tag{15}$$

Here we have that $\tilde{\mathbf{f}}_\lambda(\cdot) = [\mathbf{h}_{dc}^T(\cdot) \ \mathbf{f}_G^T(\cdot) \ \mathbf{g}_G^T(\cdot) \ \mathbf{f}_L^T(\cdot)]^T$.

From the matrix structure of $\mathbf{J}_{TS}$ and $\mathbf{J}_{PF}$, it can be shown that the right eigenvectors $\mathbf{v}$ in (14) and $\hat{\mathbf{v}}_{\tilde{z}}$ in (15) are the same up to a zero component, i.e.,

$$\hat{\mathbf{v}}_{\tilde{z}} = \begin{bmatrix} \hat{\mathbf{v}}_{x_{dc}} \\ \hat{\mathbf{v}}_{\delta_G} \\ \hat{\mathbf{v}}_{V_G} \\ \hat{\mathbf{v}}_{\delta_L} \end{bmatrix} \Rightarrow \mathbf{v} = \begin{bmatrix} \mathbf{v}_{x_{dc}} \\ \mathbf{v}_{\delta_G} \\ \mathbf{v}_{\omega_G} \\ \mathbf{v}_{V_G} \\ \mathbf{v}_{\delta_L} \end{bmatrix} = \begin{bmatrix} \hat{\mathbf{v}}_{x_{dc}} \\ \hat{\mathbf{v}}_{\delta_G} \\ \mathbf{0} \\ \hat{\mathbf{v}}_{V_G} \\ \hat{\mathbf{v}}_{\delta_L} \end{bmatrix}$$

The nonzero condition for the eigenvector can be guaranteed by requiring a particular component of $\hat{\mathbf{v}}_{\tilde{z}}$ to be equal to one ($\hat{v}_i = 1$). (Replacing $\mathbf{v} \neq \mathbf{0}$ by $\hat{v}_i = 1$ fails in the unlikely event of equations (15) yielding a nonzero eigenvector such that $\hat{v}_i = 0$.)

This technique also yields the eigenvector at the bifurcation point, offering insight into the local dynamic behavior of the system close to bifurcation, as described in [13].

An alternative method for finding the bifurcation point is to impose conditions 1 and 2 of a saddle-node to the composite function $\left[\tilde{\mathbf{f}}_\lambda^T(\tilde{\mathbf{z}}, \mathbf{u}) \ \hat{\mathbf{g}}_\lambda^T(\tilde{\mathbf{z}}, \mathbf{u})\right]^T$. This is equivalent to the approach proposed by Van Cutsem for an ac system in [18], where a Lagrangian of the reactive power flow is used to find the bifurcation. Equation (16) below defines the constraints used in this approach. Note that equations (16) are essentially the same as (15) except that the *left* zero eigenvector $\hat{\mathbf{w}}$ is used to ensure singularity.

$$\begin{bmatrix} \tilde{\mathbf{f}}_\lambda(\tilde{\mathbf{z}}, \mathbf{u}) \\ \hat{\mathbf{g}}_\lambda(\tilde{\mathbf{z}}, \mathbf{u}) \end{bmatrix} = \mathbf{0} \tag{16a}$$

$$\begin{bmatrix} \hat{\mathbf{w}}_{\tilde{z}}^T & \hat{\mathbf{w}}_u^T \end{bmatrix} \begin{bmatrix} D_{\tilde{z}} \tilde{\mathbf{f}}_\lambda & D_u \tilde{\mathbf{f}}_\lambda \\ D_{\tilde{z}} \hat{\mathbf{g}}_\lambda & D_u \hat{\mathbf{g}}_\lambda \end{bmatrix} = \mathbf{0} \tag{16b}$$

$$\begin{bmatrix} \hat{\mathbf{w}}_{\tilde{z}}^T & \hat{\mathbf{w}}_u^T \end{bmatrix} \begin{bmatrix} \partial \tilde{\mathbf{f}}_\lambda / \partial \lambda \\ \partial \hat{\mathbf{g}}_\lambda / \partial \lambda \end{bmatrix} = K \tag{16c}$$

K is an arbitrary nonzero scalar (such as $K = -1$), and

$$\frac{\partial \tilde{f}_{\lambda_i}}{\partial \lambda} = \begin{cases} \Delta P_l & \text{if } \tilde{f}_{\lambda_i} = f_{L_l} \\ 0 & \text{otherwise} \end{cases}$$

$$\frac{\partial \hat{g}_{\lambda_i}}{\partial \lambda} = \begin{cases} \Delta Q_l & \text{if } \hat{g}_{\lambda_i} = g_{L_l} \\ 0 & \text{otherwise} \end{cases}$$

Equation (16c) is equivalent to (9) for the reduced system differential equations (8), assuming $D_u \hat{\mathbf{g}}_{\lambda_0}(\tilde{\mathbf{z}}_0, \mathbf{u}_0)$ is nonsingular and exploiting the matrix structure of $\mathbf{J}_{TS}$ and $\mathbf{J}_{PF}$. See the Appendix for a formal proof of this statement.

The constraint equations defined above may have several solutions, indicating that the system model could have different parameter values yielding several bifurcation points. However, since a Newton-Raphson method is employed for finding the bifurcations, a good starting guess for the eigenvectors typically puts the initial condition within the region of attraction of the desired solution. A technique to obtain this initial guess and the computational issues involved in applying the Point of Collapse method are discussed later.

Because the system model represents limits (and hence has discontinuous derivatives), it is necessary to check whether a controller limit has been exceeded at the bifurcation point solution. HVDC converter transformer tap changers can also be included in the analysis, although several studies carried out by the authors have shown that these elements do not have a significant effect in the bifurcation point due to its limited voltage control range (see example in the next section). Nevertheless, the equation structure can be changed in these cases to reflect switches in current controllers and transformer taps, so that further analyses of the stability of the new equilibrium can be carried out.

VOLTAGE PROFILES AT BIFURCATION FOR A SAMPLE SYSTEM

Figure 3 depicts the reduced ac/dc system examined in this section. This system is a steady-state equivalent at the three buses of interest of the interconnected power systems in the western part of the United States. Generator G_2 supports the voltage at the intermediate load bus, and bus 1 has relatively strong voltage support from generator G_1. The effective short circuit ratio (ESCR) at bus 1 is 6.2, while the ESCR at the inverter side is 4.0. The dc line is designed to supply about two thirds of the power needed at bus 3, and the initial load at bus 2 is $P_L^0 = 475$ MW and $Q_L^0 = 156.1$ MVAR. Tables 1 and 2 depict all the ac/dc test system data, with generators simulated as constant voltage sources.

For variations in the load at bus 2, a computer assisted symbolic algebra package [19, 20] was used to obtain profiles for the three bus voltage magnitudes shown in Figs. 4

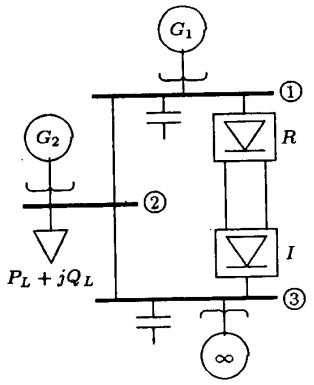

Fig. 3: *Sample ac/dc system*

through 7. Figures 4 and 5 show the "nose" curves (bifurcation diagrams) for changes in the power demand at bus 2, when VDCOLs are not considered. Full dynamic analysis shows that the equilibria with voltage magnitudes higher than those at the point of collapse (saddle-node bifurcation) are stable, whereas equilibria with voltages below this point are unstable. Figure 4 shows three additional bifurcation points in the unstable region, and also sharp turning points due to changes in the control modes of the HVDC link. This behavior is different from the behavior of an ac only system (at least for the type of ac model employed here), since in such systems the expected shape of the "nose" curves is approximately globally quadratic as shown in [21] (similar to the profiles depicted in Figs. 5 and 7). The unique character of the combined ac and HVDC system is more evident when VDCOLs are included as shown in Figs. 6 and 7. Here the ac/dc system has a completely different set of unstable equilibria, suggesting that significant changes in the stability region of the ac/dc system have taken place; also, the points of collapse have changed, i.e., the loadability margin of the system is altered by the inclusion of VDCOLs.

All these figures, especially 4 and 6, show that the stable equilibrium region of bus voltage V_1 remains approximately constant throughout the system loading, due to the relatively strong voltage support from generator G_1 and the HVDC filtering system. Hence, the VSF (dV/dQ) criteria is not a good measure of proximity to voltage collapse in this case since its value remains almost unchanged during most of the study.

Table 3 shows the values of system variables at the point of collapse, obtained by solving equations (15) for active and reactive power at the system load. For the case where VDCOLs are not included, the voltage magnitudes at bifurcation are higher when collapse is reached via active load increase as compared to reactive increase, which is reasonable due to the high reactive demands in the latter case. Although the points of collapse do not change significantly when VDCOLs are included, finding the unstable equilibrium point becomes more difficult since the controller current order changes with the ac voltage. Nevertheless, finding the bifurcation points with the PoC method is straight forward. This makes the method very appealing when compared to other methods that need to calculate the unstable

Element	G	B	$-B_s$
Line 1–2	3.68	54.13	4.68
Line 2–3	3.68	54.13	4.68
Transf. G_1		166.67	
Transf. G_2		100.00	
Transf. ∞		100.00	
Capac. 1			13.00
Capac. 3			13.68

Table 1: *AC transmission system data. All quantities are in p.u. for a 550 kV and 100 MVA base.*

Variable	Rectifier	Inverter
a	1.7634	1.7678
X_c	0.1345	0.1257
α_{min}	5^0	$\sim 120^{0\dagger}$
α_{max}	120^0	$\sim 142^{0\dagger}$
γ_{min}	$\sim 40^{0\dagger}$	18^0
γ_{max}	$\sim 155^{0\dagger}$	40^0
I_o	1.0	0.9
$I_{o_{min}}$ ‡	0.1	0.0
$V_{ac_{max}}$ ‡	0.95	0.95
$V_{ac_{min}}$ ‡	0.5	0.5
R_d	0.0624	—

†Assuming $\mu \approx 20^0$ ‡VDCOL

Table 2: *DC system data. All quantities are in p.u. for a 550 kV and 2.5 kA base.*

equilibrium points (e.g., [8]), since the degree of difficulty has not changed in the PoC method with the mode of operation of the HVDC system.

Based on the bifurcation values for active power load, the system has a large "maximum loadability" due in part to the infinite bus and the transmission line design. The active load changes are supplied mainly by the infinite bus, whereas the reactive increase is supported by the generators at buses 1 and 2; this in part explains the smaller reactive bifurcation values. Note that although the loadability margin changes when VDCOLs are included, one cannot draw a definite conclusion regarding the advantages or disadvantages of this mode of operation from the point of view of saddle-node bifurcations.

High level control modes for the HVDC system (e.g., power modulation) and transformer tap changers can easily be included in the PoC method. The idea is to find the initial bifurcation point without enforcing limits, check whether any limits have been violated, and then reapply the method to find the new saddle-node. The effect of taps in the converter transformers was simulated assuming a $\pm 10\%$ regulating range for the system in Fig. 3, obtaining a 1% variation in the bifurcation point.

Another interesting characteristic of the sample ac/dc system relates to the behavior of the eigenvalues before bifurcation. As shown in Fig. 8, a complex conjugate pair crosses the imaginary axis as the system load increases (at 4682 MW of additional load), this happens even before the system becomes unstable due to voltage collapse. This phenomenon is known as Hopf bifurcation and is described with more detail in a later section.

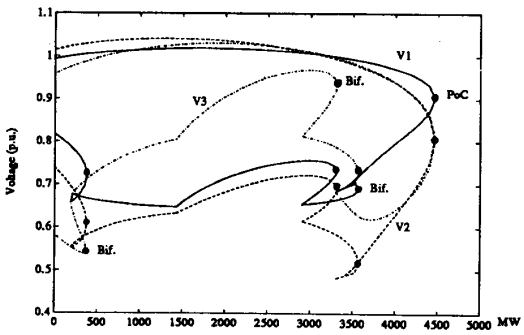

Fig. 4: *AC voltage profiles for active power changes at load bus 2 ($\Delta P_2 = 1$, $\Delta Q_2 = 0$). No VDCOL.*

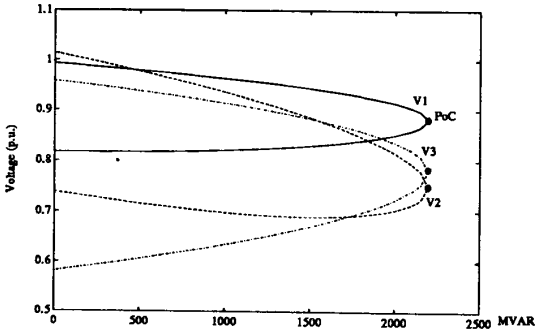

Fig. 5: *AC voltage profiles for reactive power changes at load bus 2 ($\Delta P_2 = 0$, $\Delta Q_2 = 1$). No VDCOL.*

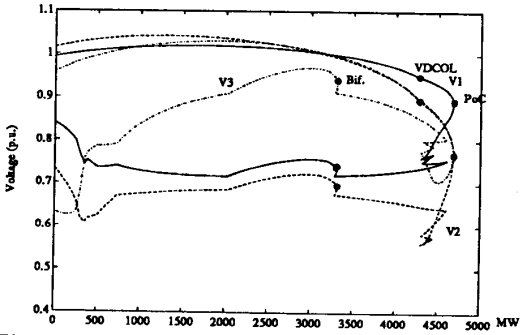

Fig. 6: *AC voltage profiles for active power changes at load bus 2 ($\Delta P_2 = 1$, $\Delta Q_2 = 0$). VDCOL included.*

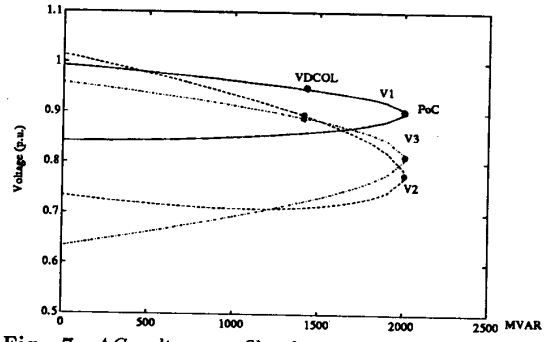

Fig. 7: *AC voltage profiles for reactive power changes at load bus 2 ($\Delta P_2 = 0$, $\Delta Q_2 = 1$). VDCOL included.*

Var.	ΔP_L No VDCOL	ΔQ_L No VDCOL	ΔP_L VDCOL	ΔQ_L VDCOL
λ	44.66	21.96	46.84	20.05
δ_1	-43.6^0	84.7^0	-44.5^0	84.2^0
δ_2	-66.1^0	58.7^0	-75.0^0	58.7^0
δ_3	-6.0^0	29.1^0	-8.1^0	29.1^0
δ_{g_1}	-28.2^0	$100.^0$	-28.9^0	99.7^0
δ_{g_2}	-62.8^0	62.3^0	-71.4^0	61.1^0
V_1	0.904	0.882	0.889	0.902
V_2	0.812	0.749	0.766	0.778
V_3	0.802	0.782	0.773	0.812
I_d	1.000	1.000	0.878	0.904
V_{d_r}	1.763	1.717	1.705	1.792
V_{d_i}	1.701	1.655	1.650	1.735
α_r	28.5^0	28.5^0	30.9^0	27.4^0
γ_i	18.0^0	18.0^0	18.0^0	18.0^0

Table 3: *Points of collapse for $V_{g_1} = V_{g_2} = V_{g_3} = 1$. Voltages and currents are in p.u., with $V_n = 550$ kV, $I_n = 2.5$ kA, and $S_n = 100$ MVA.*

COMPUTATIONAL ISSUES

One of the main concerns when applying the Point of Collapse method is the singularity of the power flow Jacobian at the bifurcation point, which might lead one to believe that equations (16) or (15) are ill-conditioned with respect to a Newton-Raphson solution algorithm. Let $\mathbf{F}(\cdot) = [\hat{\mathbf{f}}^T(\cdot)\ \hat{\mathbf{g}}^T(\cdot)]^T$ and $\mathbf{y} = [\tilde{\mathbf{z}}^T\ \mathbf{u}^T]^T$, then equations (16) become:

$$\begin{aligned} D_y\mathbf{F}^T(\mathbf{y},\lambda)\hat{\mathbf{w}}_y &= \mathbf{0} \\ \mathbf{F}(\mathbf{y},\lambda) &= \mathbf{0} \\ \frac{\partial \mathbf{F}}{\partial \lambda}^T \hat{\mathbf{w}}_y &= K \end{aligned} \tag{17}$$

Now, since $\mathbf{F}(\mathbf{y},\lambda)$ is linear with respect to λ, the Jacobian $\mathbf{J}_{PoC}$ of equations (17) is:

$$\mathbf{J}_{PoC} = \begin{bmatrix} D_y^2\mathbf{F}^T\hat{\mathbf{w}}_y & D_y\mathbf{F}^T & \mathbf{0} \\ D_y\mathbf{F} & \mathbf{0} & \frac{\partial \mathbf{F}}{\partial \lambda} \\ \mathbf{0} & \frac{\partial \mathbf{F}}{\partial \lambda}^T & 0 \end{bmatrix} \tag{18}$$

Although the individual block $D_y\mathbf{F}(\mathbf{y}_0,\lambda_0)$ is singular, conditions (9) and (10) imply that $\mathbf{J}_{PoC}$ is nonsingular [22].

The Jacobian $\mathbf{J}_{PoC}$ is symmetric for an ac lossless system [18], and topology-symmetric for a general ac system. However, the equations for the HVDC links cause the power flow Jacobian to be rather unsymmetric. Furthermore, for an ac system this Jacobian has an special structure that can be exploited using blocking techniques to reduce the computational burden [18], but once the dc system is included in the analysis this structure is partially lost. Nevertheless, one can still use matrix blocking techniques to improve the computational characteristics of the proposed method.

An important issue in solving the Point of Collapse equations by Newton's method is the choice of initial guess for eigenvectors $\hat{\mathbf{v}}_y$ or $\hat{\mathbf{w}}_y$. The approach used here is to apply several iterations of the Inverse Power Method [23] to the power flow Jacobian. This typically yields a vector close to the span of the real and imaginary parts of the eigenvector(s) corresponding to the eigenvalue(s) with the smallest magnitude. Although this is not absolutely guaranteed to

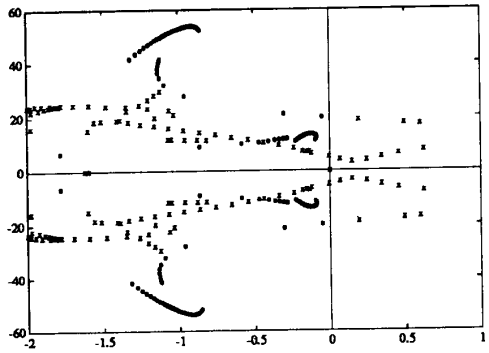

Fig. 8: *Eigenvalues for the stable (o) and unstable (x) equilibria for active power changes at bus 2. VDCOL included.*

be the eigenvalue that eventually goes to zero at bifurcation, it is quite likely. The method has proven effective in a number of sample ac and ac/dc systems, and often produces a good initial guess in just one iteration.

With a proper initial guess, the computational costs of solving (15), or (16) are somewhat higher than those for the original power flow equations. The number of equations has doubled, but the Jacobian $\mathbf{J}_{PoC}$ retains its sparsity. Furthermore, close to the bifurcation point the power flow Jacobian $\mathbf{J}_{PF}$ becomes ill-conditioned, causing slow convergence for power flow methods and continuation methods [21], whereas the Jacobian for the proposed Newton solution is far from singularity.

Research currently under way on computation of points of collapse using the proposed technique in systems with over 100 buses, suggests solution times in the order of 10 to 20 ordinary power flows. However, more work has to be done on this area before reaching definite conclusions.

HOPF BIFURCATIONS

Hopf bifurcation is another mechanism of transition to instability in dynamical systems. This phenomenon is characterized by complex eigenvalues of the linearized system dynamics crossing the imaginary axis as the system parameters change [11, 12]. This type of bifurcation has been proven not to exist for simple ac lossless system models [24]. However, it has been observed in more detailed ac system models that consider transfer conductances and exciter dynamics [25].

These bifurcations were observed for the ac/dc system examined here, as shown in the eigenvalue-locus of Fig. 8 obtained when the active power at bus 2 is increased and VDCOLs are included. Here complex conjugate eigenvalues of a stable equilibrium crosses the imaginary axis from left to right, slightly before the system reaches a saddle-node. This makes the system unstable by a different mechanism than voltage collapse. The interested reader is referred to [26] for a description of computational techniques for finding these bifurcations in nonlinear power system models.

CONCLUSIONS

A thorough analysis of bifurcation phenomena in a particular model of ac/dc systems is presented. The Point of Collapse method is shown to be computational feasible as a means to determine acceptable load increase before encountering voltage collapse in ac/dc systems. Moreover, it appears particularly promising when HVDC lines with controller limits and VDCOLs are considered.

The results presented here justify further studies in larger systems of the proposed method. The authors are currently working in implementing the PoC method for arbitrary ac/dc system dimensions in a UNIX work-station environment using C code.

ACKNOWLEDGEMENTS

The support of this work by the Electric Power Research Institute project RP 2675-4 and National Science Foundation grants ECS-8857019, ECS-9009079, and ECS-8907391 is gratefully acknowledged. Also the authors would like to thank Stig Nilsson of EPRI for his valuable comments and suggestions.

REFERENCES

[1] *Proceedings: Bulk Power System Voltage Phenomena—Voltage Stability and Security*, EPRI EL-6183, Jan. 1989.

[2] *Methodology of Integration of HVDC Links in Large AC Systems—Phase 1: Reference Manual*, EPRI EL-3004, March 1983.

[3] *Methodology of Integration of HVDC Links in Large AC Systems—Phase 2: Advanced Concepts*, EPRI EL-4365, Vol. 1, April 1987.

[4] J. Arrillaga, *High Voltage Direct Current Transmission*, Peter Peregrinus Ltd., London, UK, 1983.

[5] J. Arrillaga, C. P. Arnold, B. J. Harker, *Computer Modelling of Electrical Power Systems*, John Wiley & Sons, UK, 1983.

[6] A. E. Hammad and W. Kuhn, "A Computation Algorithm for Assessing Voltage Stability at AC/DC Interconnections," *IEEE Trans. Power Systems*, Vol.1, No. 1, Feb. 1986, pp. 209–216.

[7] B. Frankén and G. Andersson, "Analysis of HVDC converters connected to Weak AC Systems," *IEEE Trans. Power Systems*, Vol. 5, No. 1, Feb. 1990, pp. 235–242.

[8] Y. Tamura, K. Sakamoto and Y. Tayama, "Current Issues in the Analysis of Voltage Instability Phenomena," pp. 5.39–5.53 in [1].

[9] C. L. DeMarco, T. J. Overbye, "An Energy Based Security Measure for Assessing Vulnerability to Voltage Collapse," *IEEE Trans. Power Systems*, Vol.5, No. 2, May 1990, pp. 419–427..

[10] W. Rudin, *Principles of Mathematical Analysis*, Third Edition, McGraw-Hill, USA, 1976.

[11] J. Guckenheimer and P. Holmes, *Nonlinear Oscillations, Dynamical Systems, and Bifurcations of Vector Fields*, Springer-Verlag, New York, USA, 1986.

[12] R. Seydel, *From Equilibrium to Chaos—Practical Bifurcation and Stability Analysis*, Esevier Science Publishers, North-Holland, 1988.

[13] I. Dobson and H. D. Chiang, "Towards a Theory of Voltage Collapse in Electric Power Systems," *Systems & Control Letters 13*, 1989, pp. 253–262.

[14] H. G. Kwatny, "Steady State Analysis of Voltage Instability Phenomena," pp. 5.1–5.22 in [1].

[15] S. Sastry and P. P. Variaya, "Hierarchical Stability and Alert State Steering Control of Interconnected Power Systems," *IEEE Trans. Circuits and Systems*, Vol. 27, No. 11, Nov. 1980, pp. 1102–1112.

[16] P. W. Sauer and M. A. Pai, "Power System Steady-State Stability and the Load Flow Jacobian," *IEEE/PES 89 SM 682-6 PWRS*, July 1989.

[17] F. L. Alvarado and T. H. Jung, "Direct Detection of Voltage Collapse Conditions," pp. 5.23–5.38 in [1].

[18] T. Van Cutsem, "A Method to Compute Reactive Power Margins with respect to Voltage Collapse," *IEEE/PES 90 WM 097-6 PWRS*, Feb. 1990.

[19] F. L. Alvarado, *Solver-Q Instruction Manual*, Software Development Distribution Center, University of Wisconsin-Madison, 1987.

[20] F. L. Alvarado and D. J. Ray, "Symbolically-assisted Numeric Computation in Education," *Int. J. Appl. Engr. Ed.*, Vol. 4, No. 6, pp. 519–536, 1988.

[21] K. Iba, H. Suzuki, M. Egawa and T. Watanabe, "Calculation of Critical Loading Condition with Nose Curve Using Homotopy Continuation Method," *IEEE/PES 90 SM 415-0 PWRS*, July 1990.

[22] A. Spence and B. Werner, "Non-simple Turning Points and Cusps," *IMA J. Num. Analysis* **2**, 1982, pp. 413-427.

[23] S. D. Conte and Carl de Boor, *Elementary Numerical Analysis—An Algorithmic Approach*, Third Edition, McGraw-Hill, New York, USA, 1980.

[24] H. D. Chiang and F. F. Wu, "Stability of Nonlinear Systems Described by a Second-Order Vector Differential Equation," *IEEE Trans. Circuits and Systems*, Vol. 35, No. 6, June 1988, pp 703–711.

[25] E. H. Abed and P. P. Varaiya, "Nonlinear Oscillations in Power Systems," *International Journal of Electric Power & Energy Systems*, Vol. 6, 1984, pp. 37–43.

[26] F. L. Alvarado, "Bifurcations in Nonlinear Systems: Computational Issues," *Proceedings of ISCAS*, New Orleans, Lousiana, May 1–3, 1990, pp. 922–925.

APPENDIX: EQUIVALENCE OF SADDLE-NODE CONDITIONS

This appendix shows that (9) is equivalent to equation (16c). Let $D_u\hat{\mathbf{g}}(\cdot)$ be nonsingular at the equilibrium point $(\mathbf{z}_0, \mathbf{u}_0, \lambda_0)$ for equations (8). There exists a local function $\mathbf{h}(\cdot)$ around the equilibrium such that $\mathbf{u} = \mathbf{h}(\mathbf{z}, \lambda)$. Then,

$$\begin{aligned} \hat{\mathbf{g}}(\mathbf{z}, \mathbf{u}, \lambda) &= \hat{\mathbf{g}}(\mathbf{z}, \mathbf{h}(\mathbf{z}, \lambda), \lambda) = \mathbf{0} \\ \Rightarrow \left.\frac{\partial \mathbf{u}}{\partial \lambda}\right|_0 &= -D_u\hat{\mathbf{g}}|_0^{-1} \left.\frac{\partial \hat{\mathbf{g}}}{\partial \lambda}\right|_0 \end{aligned}$$

On the other hand, since $\mathbf{s}(\mathbf{z}, \mathbf{u}, \lambda) = \hat{\mathbf{f}}(\mathbf{z}, \mathbf{h}(\mathbf{z}, \lambda), \lambda)$:

$$\begin{aligned} \left.\frac{\partial \mathbf{s}}{\partial \lambda}\right|_0 &= \left.\frac{\partial \hat{\mathbf{f}}}{\partial \lambda}\right|_0 + D_u\hat{\mathbf{f}}|_0 \left.\frac{\partial \mathbf{u}}{\partial \lambda}\right|_0 \\ &= \left.\frac{\partial \hat{\mathbf{f}}}{\partial \lambda}\right|_0 - D_u\hat{\mathbf{f}}|_0 D_u\hat{\mathbf{g}}|_0^{-1} \left.\frac{\partial \hat{\mathbf{g}}}{\partial \lambda}\right|_0 \end{aligned} \quad (A.1)$$

Now, from the ac/dc reduced differential equations (8) and condition 1 of a saddle-node it follows that

$$\hat{\mathbf{w}}_u^T = -\hat{\mathbf{w}}_z^T D_u\hat{\mathbf{f}}|_0 D_u\hat{\mathbf{g}}|_0^{-1} \quad (A.2)$$

$$\begin{aligned} \mathbf{0} &= \hat{\mathbf{w}}_z^T \underbrace{\left(D_z\hat{\mathbf{f}}|_0 - D_u\hat{\mathbf{f}}|_0 D_u\hat{\mathbf{g}}|_0^{-1} D_z\hat{\mathbf{g}}|_0\right)}_{D_z\mathbf{s}|_0} \\ \Rightarrow \mathbf{w} &= \hat{\mathbf{w}}_z \end{aligned} \quad (A.3)$$

Thus, from equations (A.1), (A.2), and (A.3) it can be seen that equations (9) and (16c) are equivalent, i.e.,

$$\begin{aligned} \mathbf{w}^T \left.\frac{\partial \mathbf{s}}{\partial \lambda}\right|_0 &= \hat{\mathbf{w}}_z^T \left.\frac{\partial \hat{\mathbf{f}}}{\partial \lambda}\right|_0 + \hat{\mathbf{w}}_u^T \left.\frac{\partial \hat{\mathbf{g}}}{\partial \lambda}\right|_0 \\ &= \hat{\mathbf{w}}_{\hat{z}}^T \left.\frac{\partial \tilde{\mathbf{f}}}{\partial \lambda}\right|_0 + \hat{\mathbf{w}}_u^T \left.\frac{\partial \hat{\mathbf{g}}}{\partial \lambda}\right|_0 \\ &= \hat{\mathbf{w}}_y^T \frac{\partial \mathbf{F}}{\partial \lambda} = K \neq 0 \end{aligned} \quad (A.4)$$

Similar arguments can be used to prove the equivalence of equation (10) and the corresponding saddle-node condition for the power flow equations, i.e.,

$$\mathbf{w}^T \left[D_z^2\mathbf{s}|_0\mathbf{v}\right] \mathbf{v} = \hat{\mathbf{w}}_y^T \left[D_y^2\mathbf{F}\, \hat{\mathbf{v}}_y\right] \hat{\mathbf{v}}_y \neq 0 \quad (A.5)$$

Based on (A.4) and (A.5), one can readily prove that the Point of Collapse Jacobian is nonsingular.

Claudio A. Cañizares (S'87) was born in Mexico, D.F. in 1960. In April 1984, he received the Electrical Engineer degree from the Escuela Politécnica Nacional (EPN), Quito-Ecuador, where he is currently an Assistant Professor on leave of absence, and the MSEE from the University of Wisconsin-Madison in 1988. Mr. Cañizares is a PhD student, T.A., and R.A. at the University of Wisconsin-Madison, sponsored by Fulbright, OAS, and EPN.

Fernando L. Alvarado (M'69, SM'78) was born in Lima, Peru. He received the BEE and PE degrees from the National University of Engineering in Lima, Peru, the MS degree from Clarkson University, and the PhD degree from the University of Michigan in 1972. Since 1975 he has been with the University of Wisconsin in Madison, where he is a Professor of Electrical and Computer Engineering.

Christopher L. DeMarco (S'80, M'85) was born in Derby, Connecticut in 1958. He received his Bachelor of Science degree in Electrical Engineering from the Massachusetts Institute of Technology in June of 1980, and his PhD degree in Electrical Engineering and Computer Sciences from the University of California, Berkeley in May 1985. In January 1985, he joined the faculty of the Department of Electrical and Computer Engineering at the University of Wisconsin-Madison.

Ian Dobson (M'89) received the BA in Mathematics from Cambridge, England and the PhD in Electrical Engineering from Cornell and he joined the University of Wisconsin-Madison faculty in 1989. His industrial experience included writing a general simulation of switching power supplies and his current interests include voltage collapse in electric power systems and applications of nonlinear dynamics and bifurcation theory.

Willis F. Long (M'69, F'89) received his B.Sc. and M.Sc. in Engr. Physics and EE from the Univ. of Toledo, and the PhD in EE from the Univ. of Wisconsin-Madison in 1970. He was a technical staff member at Hughes Research Labs. and Director of ASEA Power Systems Center, New Berlin, WI. Since 1973 he has been on the faculty of the Univ. of Wisconsin-Madison. Dr. Long's research interests are in the analysis and simulation of HVDC transmission systems.

Discussion

Adam Semlyen (University of Toronto): I would like to commend the authors for their interesting and timely paper. It extends the powerful method for the direct computation of the point of collapse to AC/DC power systems. I find it significant that the authors have included in their analysis the modeling of connected components for all buses, i.e., for generators, loads, and converters. Equations (8) reflect this fact by their generality. The power flow Jacobian examined in the sequel has, I believe, a similarly general interpretation by fully reflecting the effects of terminal components. This, however, is not the case with the power flow Jacobian $\mathbf{J}_{PF}$ as it is usually defined in the literature.

On occasion, engineers who found that a power flow program, in particular Newton-Raphson, did not converge, attributed this fact to the (voltage) instability of the system. Therefore, attention was initially focused on the Jacobian of the standard power flow formulation, when problems of voltage stability had to be examined. In conventional power flow, buses are characterized as *P-V* and *P-Q*, which implies that $\mathbf{J}_{PF}$, the power flow Jacobian, does not reflect load and generator characteristics. Yet some of the earlier assessments of proximity to the point of collapse were based on the examination of the closeness to singularity of this $\mathbf{J}_{PF}$. It is quite clear that this view is oversimplified. Figure 1 illustrates this by means of system and load characteristics represented at a particular load bus.

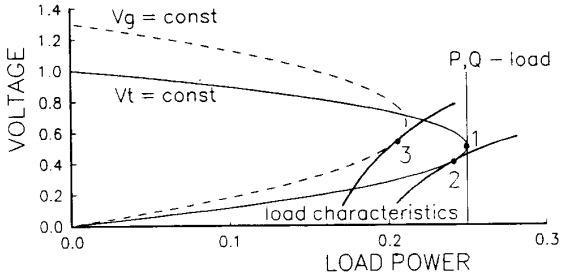

Fig.1 Illustration of the effect of system and load characteristics on the resultant bifurcation points, 1, 2, and 3.

If the generator bus voltage V_t is assumed constant and the load power is assumed not to depend on voltage, then the critical point is 1, where P and Q are maximal. This point corresponds to $\mathbf{J}_{PF}$ being singular. If a voltage dependent load characteristic is considered, as in equations (3) of the paper, then the bifurcation point is 2 on the V_t = constant curve, and 3 on the (internal generator voltage) V_g = constant curve. There are, of course, appropriate Jacobians $\mathbf{J}_{adj}$ that can be obtained by adjusting the diagonal elements of the four blocks of $\mathbf{J}_{PF}$ and that become singular at the bifurcation points 2 and 3. However, it is appropriate to make a clear distinction between the two Jacobians, $\mathbf{J}_{PF}$ and $\mathbf{J}_{adj}$, when analyzing the singularities of the full linearized dynamics of the system. It seems that often the discussions in the literature, related to this topic, focus on $\mathbf{J}_{PF}$ and have therefore little chance of producing results of general validity.

The direct method of obtaining the exact point of collapse, described in the paper, is of significance since it is indeed difficult to get very close to the point of collapse using conventional power flow programs. (However, by appropriate choice of the load characteristics, the critical loading point can be reached; see the closure of [21].) The computing time of 10 to 20 times that for ordinary power flows, mentioned in the paper, suggests that the Newton-Raphson method may not be the best choice for solving the point of collapse problem, possibly because of the second order derivatives in Jacobian (18). Would an approximation to the Jacobian (with, however, accurate mismatches) not lead to faster solutions, similarly to the fast decoupled load flows? For instance, starting with equations (14), and denoting $\{\mathbf{z}, \lambda\}$ by ξ ($\in \mathbf{R}^{n+1}$) and setting $\mathbf{v} = [1 \ \eta^T]^T$ ($\eta \in \mathbf{R}^{n-1}$), we get

$$s(\xi) = 0 \qquad (a_1)$$
$$a(\xi) + A(\xi)\eta = 0 \qquad (a_2)$$

where a is the first column and A the remainder of the Jacobian of (14). Since (a_2) is linear in η, the Jacobian of equations (a) can be *approximated* by

$$\begin{bmatrix} \frac{ds}{d\xi} & 0 \\ \frac{da}{d\xi} & A \end{bmatrix} \qquad (b)$$

where susceptances B can be used as further approximations. Matrix (b) is bloc triangular and sparse, and has common elements in its blocks. My guess for the solution time is that it could be of the order of that needed for two fast decoupled load flows.

The authors' comments on the above issues would be much appreciated.

Manuscript received August 14, 1991.

M. K. Pal (Public Service Electric and Gas Company, Newark, N.J.): This paper actually describes a method to determine the maximum power point as determined by network laws. The authors appear to imply that this is also the voltage stability limit or the point of collapse. We would, however, have serious reservations about the applicability of the methodology to the voltage stability issues. Our concerns are based on the following observations.

Voltage stability is load driven. A valid dynamic load model is, therefore, essential in any voltage stability analysis. The model used by the authors (equation 3) is really a static model, as far as voltage stability is concerned. This may not be apparent until its pertinence to voltage stability is properly examined. The term involving the load frequency has little bearing on voltage collapse. Actually, since δ_L is not a state variable (in the system formulation normally employed in network and stability analyses, such as the one used by the authors, it can have discontinuities), the use of δ_L in equations (3) and (7) is not valid. It is not difficult to show the problems one can get into in voltage stability studies, if the load model contains terms involving δ_L's. Also, although a term is included in the load model to simulate the slow time scale load variation, it does not make the model a valid dynamic model. It simply signifies the change in the load level with time. The load model remains static from the viewpoint of voltage stability. Such terms may have some significance in the determination of power limit and the point in time at which it occurs, without regard to voltage stability.

It can be shown that the load model of equation (3) of the paper, after omitting the frequency term for the reason stated above, cannot cause voltage instability, as determined by applying the accepted criteria of stability of dynamic systems, when generators are simulated as constant voltage sources, as done by the authors in their example. With generators simulated as indicated in equation (1) of the paper, the eigenvalue analysis will show a stable region, followed by an unstable region and then another stable region, as one follows the "nose" curves, even in purely ac systems. Using only the voltage dependent terms in the load model, no voltage instability would be encountered.

Contrary to what the authors claim, the relationship between the singularity (zero eigenvalue) of the power flow (or any other) Jacobian and a zero eigenvalue of the linearized dynamic system has not been demonstrated in the paper. If the frequency term is removed from the load model, and the analysis is repeated, it is not difficult to see that when the power flow Jacobian becomes singular, the denominator in the right-hand side of equation (13) of the paper also becomes zero. Singularity of the power flow Jacobian, therefore, provides no indication of the stability status of the dynamic system. References [14-16] of the paper suffer from the same basic problem. In [A], it is shown that when the loads are represented by static models, and the generator flux linkage dynamics are neglected, there cannot be voltage instability. Singularity of the power flow Jacobian signifies a power limit as determined by network laws.

When flux dynamics are included in the model, the results for constant power static load model will be anomalous, as pointed out earlier. A realistic dynamic model of the constant power load will, however, show that, in the absence of excitation control, the voltage stability limit is determined by the generator internal voltage behind synchronous reactance, i.e. the field voltage, if the saliency is neglected. Since the authors' model does not include the exciter dynamics, the inclusion of the equation representing generator transient voltage dynamics is inconsequential. It will have no effect on the voltage stability limit. Also note that the expressions for the generator power

outputs, as given in the paper, implies that $x_q = x_d'$. In general, x_q is four to six times the value of x_d'.

From the above discussion it should be clear why the complex conjugate eigenvalues crossing the imaginary axis have nothing to do with voltage instability. Obviously, it was caused by the HVDC dynamics, assuming there was no programming error. It is not clear why the equilibrium was labeled "stable" when this happened, although the system is clearly unstable.

Voltage instability can only be caused by loads that tend to restore to constant MVA, either due to the nature of the load itself, or due to the action of some control mechanism, such as LTCs, which tend to maintain constant voltage, thereby rendering any load constant MVA. A pertinent dynamic model of such loads is necessary in order to properly address the voltage stability problem. Depending on the type of load, and in the case of constant MVA loads their speed of response, voltage stability limit can be anywhere from well below the power limit as indicated by the singularity of the Jacobian to well into the low voltage solution region.

[A] M. K. Pal, Discussion of "An Investigation of Voltage Instability Problems," by N. Yorino, H. Sasaki, Y. Masuda, Y. Tamura, M. Kitagawa and A. Oshimo, 91 WM 202-2 PWRS, IEEE/PES winter meeting February, 1991.

Manuscript received August 26, 1991.

C. A. Cañizares*, F. L. Alvarado, C. L. DeMarco, I. Dobson, W. F. Long (*Escuela Politécnica Nacional–Quito, University of Wisconsin–Madison): The authors appreciate the interest demonstrated by the discussers in the paper. With regard to the comments by Professor Semlyen, he is certainly right when pointing out that the power flow utilized in the paper should not correspond to the standard power flow mismatch equations; these equations cannot be used to reliably detect singularities in the Jacobian of the dynamic equations. In the paper we used an "extended" power flow that predicts the steady state of the complete set of dynamic equations. Then, based on a generic assumption of nonsingularity of the algebraic equation Jacobian, these equations are used to detect a bifurcation (singularity) point.

The second issue raised by Dr. Semlyen, and also raised by Mr. Pal, corresponds to the dynamic load model used in the paper. The paper utilizes well known transient stability models for generators, transmission lines and loads [3, 5]; the original research effort concentrated on the DC system, which was viewed as a special kind of dynamic load. The methodology presented in the paper, treating saddle-node bifurcations of dynamic systems with algebraic constraints, certainly holds for other load models as well as for other generator models. In the example presented in the paper, the bifurcation point is the same as the maximum power transfer point, i.e., the tip of the P-V curves, because the load change was modeled only with variation in the constant powerterm. However, a different load model (e.g., a mixture of constant power and constant impedance) might produce a different result; in this case the bifurcation diagram, would not necessarily correspond to a P-V curve. This can be easily demonstrated in the simple circuit of Fig. A1, where a constant power increment produces a bifurcation of the system dynamics at the tip of the P-V curve; nevertheless, if one uses a constant impedance model for the load, the system does not present any bifurcation for any value of R, although the P-V curves are the same in both cases. Furthermore, in this case all points of the P-V curve are stable. This result somewhat corroborates one of Mr. Pal's comments, and is a well established result in the area of voltage stability [A4].

We have considered the possibility of using different techniques to accelerate the solution of the PoC method, although not exactly like the one proposed by Prof. Semlyen. However, these techniques did not give good results, especially when dealing with large systems. In larger systems, the improved convergence characteristics given by using the full Jacobian of the Newton-Rapson based PoC method have proven very important to obtain a solution to the PoC problem. Good algorithms for choosing initial conditions for this iteration have also proven important for convergence.

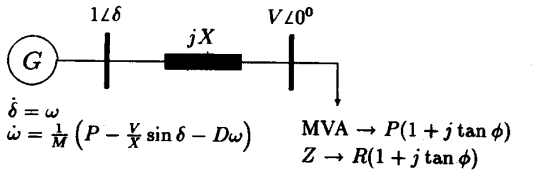

Fig. A1: *Simple generator-line-load power system model.*

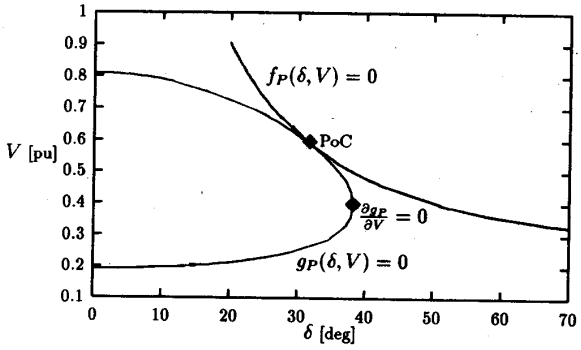

Fig. A2: *Active and reactive power constraints $f_P(\delta, V) = 0$ and $g_P(\delta, V) = 0$, respectively, for the power system of Fig. A1 at the bifurcation point (P=0.6180). The data used for this system are: $X = 0.5$, $\tan\phi = 0.5$, $H = 19$, $D = 0.1$.*

Regarding Mr. Pal's criticisms, we would like to address each of them to clarify what seems to be a misunderstanding of the main ideas presented in the paper. We believe that most of Mr. Pal's comments are based on his doubts that voltage collapse problems are related to a saddle-node bifurcation phenomena, as one gathers from his remarks in paragraph four of the discussion. On this issue we refer the discusser to the work by Dobson and Chiang [13] and also by Kwatny [14], and many other authors [A1, A2]. We also would like to encourage Mr. Pal to solve the simple system of Fig. A1 himself. In this system one can easily show that for a simple constant power load model, where there is no dynamic frequency dependent term on the load and the generator is modeled as a constant voltage source, singularity of the dynamic equations' Jacobian occurs at the same point where the power flow Jacobian becomes singular without having a singular algebraic constraint, contrary to what Mr. Pal suggests on paragraphs three and four of his discussion. This can be clearly observed in Fig. A2. In this circuit one can also show by a simple dynamic simulation that at this bifurcation point the voltage at the load bus collapses. We have made the same observations in ac/dc and ac-only dynamic systems of up to 173 buses. Furthermore, in all the cases where the load was simulated as constant power, the P-V curve have all stable equilibrium points above the bifurcation point, whereas the equilibrium points on the other side of the nose curve are

unstable of type 1, just as predicted by bifurcation theory. This was determine by using standard eigenvalue computation packages (i.e., Matlab [A5]), and the same was done for the example shown in the paper.

As far as the generator model is concern, it is a model directly extracted from [13,15]. It represents a synchronous machine with round rotor where only the d-axis transient effects are considered. This is what Arrillaga denotes as model 2 in his book [15]. The equations presented in the paper are consistent with this established text. Since this was not the main concern of the paper, we did not study the influence of the transient voltage equation in the bifurcation phenomena. Nevertheless, Mr. Pal's reasoning to argue that this equation has no influence at all in the saddle-node bifurcation point does not suffice to support his definite assertions.

Mr. Pal is right when commenting that the Hopf bifurcations observed in the example are due to the HVDC link, and this is clearly stated as one of the conclusions of the paper. Such instabilities can also be observed when fast automatic voltage regulators are added to the generator [25]. However, the Hopf bifurcation section of the paper clearly states that this phenomena is not considered a voltage *collapse* problem. On the contrary, it is identified as a completely different mechanism of instability. Furthermore, these points are clearly identified in Fig. 8 as obviously unstable. As to whether this is a voltage stability problem, we certainly believe it is, since it produces large and undesirable voltage oscillations as shown in [A3]. But it does not lead to monotonic decline of voltage magnitudes, so we can choose not to classify it as voltage *collapse*.

Finally, we think that not only constant MVA loads produce voltage instability in power systems, as Mr. Pal suggests on his last paragraph. HVDC links, as shown in the paper, and voltage regulators are certainly other sources of voltage stability problems. Furthermore, loss of reactive support from generation could also drive the system to voltage collapse. We certainly agree with Dr. Semlyen and Mr. Pal in that better dynamic models of the load are needed, and this is one of the main concerns of many researchers currently working in the field.

[A1] C. Barbier and J-P. Barret, "An Analysis of Phenomena of Voltage Collapse on a Transmission System," *Revue Generale de l'electricite*, Vol. 89, October 1980, pp. 672–680.

[A2] M. M. Begovic and A. G. Phadke, "Dynamic Simulation of Voltage Collapse," *IEEE Trans. Power Systems*, Vol. 5, No. 1, February 1990, pp. 198–203.

[A3] L. A. S. Pilotto, M. Szechtman, A. E. Hammad, "Transient AC Voltage Related Phenomena for HVDC Schemes Connected to Weak AC Systems," *IEEE/PES 91 SM 305-3-PWRD*, July 1991.

[A4] C. Rajagopalan, B. Lesieutre, P. W. Sauer and M. A. Pai, "Dynamic Aspect of voltage/Power Characteristics," *IEEE/PES 91 SM419-2 PWRS*, San Diego, CA, July 28–August 1 1991.

[A5] C. Moler, J. Little and S. Bangert, "Matlab User's Guide," The Mathworks, Inc., Sherborn, MA, 1987.

Manuscript received November 14, 1991.